THE JOURNAL OF PHYSICAL CHEMISTRY B

Article

pubs.acs.org/JPCB

# On the Origin of Thermal Untwisting of DNA

Alexey K. Mazur*

Institut de Biologie Physico-Chimique, UPR9080 CNRS, Univ Paris Diderot, Sorbonne Paris Cité, 13 rue Pierre et Marie Curie, Paris 75005, France

Supporting Information

**ABSTRACT:** In aqueous solutions, the helical twist of DNA decreases with temperature. This phenomenon was noticed and studied experimentally several decades ago, but its physical origin remains elusive. The present paper shows that the thermal untwisting can be predicted from the specific properties of the torsional elasticity of the double helix revealed in recent computational studies. The temperature coefficient of untwisting estimated using coarse-grained models fitted to all-atom MD data accounts for the experimental results nearly quantitatively. The agreement is further improved with the computed torsional rigidity scaled to remove the discrepancy from experiment. The results confirm that the torsional rigidity of DNA is strongly anharmonic. They indicate that for random DNA, its value grows with small twisting and decreases with untwisting.

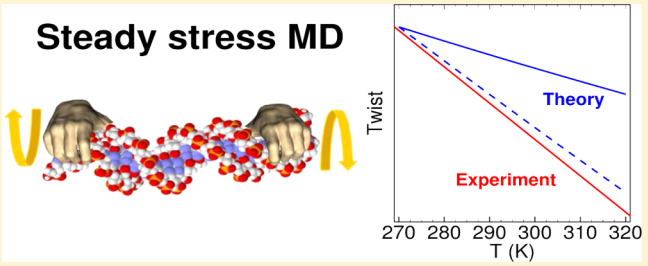


## INTRODUCTION

The double-helical DNA is a twist-storing polymer, that is, it responds to the torsional stress elastically by deviating from an equilibrium twist and coming back when the stress is relaxed. In living cells, DNA is often required to be temporarily twisted so that surface sites separated by many base pair steps (bps) are properly oriented.[1] The twisting is commonly coupled to bending, and to understand these processes, one needs to know the forms and parameters of the corresponding potentials. Many essential properties of long DNA are well described by the harmonic worm-like rod (WLR) model.[2,3] However, this is just because the additivity of local fluctuations and the central limiting theorem make any long twistable polymer statistically equivalent to a harmonic WLR. The local twisting in DNA cannot be harmonic because the double helix is chiral and the twisting is not a mirror image of untwisting. In the linear approximation, this leads to asymmetric coupling between twisting, bending, and stretching.[3−7] In the next approximation, the twisting rigidity of DNA should vary with the superhelical density, for instance, and even a small local nonlinearity is essential because biologically relevant fluctuations are large. All-atom molecular dynamics (MD) simulations revealed that, depending on the base pair sequence, the torsional rigidity may grow or decrease with twisting.[8,9] Experimentally, this effect was earlier probed only by the fluorescence polarization anisotropy (FPA) method.[10−13] It was found that the twisting rigidity of DNA depends on supercoiling, but the conclusions concerning the form of this dependence were controversial. The sign and the magnitude of this effect in random DNA remain uncertain. To shed light upon this issue, we examined other potentially relevant observations. One of them is the temperature dependence of the average twist of free DNA.

It is long known that in aqueous solutions, the helical twist of DNA decreases with temperature. This property was discovered several decades ago[14−16] and used for producing positive supercoils in circular plasmids.[17] The physical origin of this phenomenon is elusive. To my knowledge, the only qualitative interpretation was proposed in the study of DNA untwisting by organic cosolvents.[18] It was known that moderate heating causes the growth of the buoyant density of DNA in CsCl probably due to the loss of hydration water.[19] Lee et al. hypothesized that dehydration causes untwisting and that organic cosolvents dehydrate DNA.[18] This interpretation has some doubtful points. Notably, there is no structural model of how the reduced activity of water can untwist DNA. Just renaming the untwisting from "thermal" to "dehydration" does not change much. On the other hand, any change in the structure of DNA may alter the number of strongly bound water molecules. The loss of DNA-bound water in CsCl can be a consequence rather than the cause of untwisting. Moreover, both dehydration and organic cosolvents are known to stabilize the A-form of DNA (reviewed in ref 20). The A-form has lower twist, and this observation seems to support the above hypothesis. However, the specific magnitudes of untwisting[18] are anticorrelated with the ability of the corresponding cosolvents to induce the B-to-A transitions, that is, cosolvents known to strongly reduce the water activity produce less untwisting.

We surmised that the thermal untwisting can be a natural consequence of the inherent anharmonic twisting potential of DNA. In the first approximation, the twist energy profile near

Received: November 19, 2012
Revised: January 16, 2013
Published: January 18, 2013





dx.doi.org/10.1021/jp311408h | J. Phys. Chem. B 2013, 117, 1857−1861

the minimum is harmonic and the average twist cannot change with the temperature. In the next approximation, the profile is anharmonic and its left (untwisting) branch can be less steep than the right one. In this case, the heating should reduce the average twist. A less steep energy profile is a synonym of softer DNA, that is, the torsional rigidity of DNA should also decrease with untwisting. A strong anharmonicity of this type has been uncovered in MD simulations of DNA with the GC-alternating base pair sequence (GC-DNA).[8,9] We decided to check whether or not this anharmonicity can account for the experimental thermal untwisting. A brute-force approach, that is, MD simulations under different temperatures to measure the twist, is prohibitively costly. Therefore, here, we consider this problem by using multiscale modeling, that is, we try to find parameters of a WLR that would produce the pattern of torsional fluctuations identical to that of all-atom DNA in MD. The resulting coarse-grained model behaves in strict agreement with the Boltzmann's statistics; therefore, the required temperature dependence can be estimated directly without simulations. It appears that the thermal untwisting effect is reproduced, with a temperature coefficient that accounts for a significant part of the experimental dependence. Moreover, the temperature coefficient close to experiment is obtained if one takes into account that MD overestimate the twisting rigidity of DNA.

## METHODS

**MD Simulations.** All-atom tetradecamer DNA duplexes with complementary GC-alternating (GC-DNA) and AT-alternating (AT-DNA) sequences were modeled in an aqueous environment with neutralizing sodium ions. MD simulations were carried out in conditions of steady torsional stress.[8,9,21] We consider the results from our previous report[9] obtained with parm98 AMBER force field parameters[22,23] and new data for GC-DNA obtained with the recent bsc0$_{\chi OL4}$ version.[24−26] All calculations were carried out by running independent trajectories in parallel on 48 processors for identical conditions. The starting states were prepared as described in the earlier study.[9] The electrostatic interactions were treated by the SPME method,[27] with the common values of Ewald parameters, that is, 9 Å truncation for the real space sum and $\beta \approx 0.35$. The temperature was maintained by the Berendsen algorithm[28] applied separately to solute and solvent with a relaxation time of 10 ps. To increase the time step, MD simulations were carried out by the internal coordinate method (ICMD),[29,30] with the internal DNA mobility limited to essential degrees of freedom. The rotation of water molecules and internal DNA groups including only hydrogen atoms was slowed down by weighting of the corresponding inertia tensors.[31,32] The double-helical DNA was modeled with all backbone torsions, free bond angles in the sugar rings, and rigid bases and phosphate groups. The effect of these constraints was previously checked through comparisons with standard Cartesian dynamics,[31,33] and it is not significant. The time step was 0.01 ps, and the DNA structures were saved every 5 ps. All trajectories were continued to obtain the sampling corresponding to 164 ns of continuous dynamics, that is, $2^{15}$ points for every value of the applied external torque $\tau$. Statistical convergence and errors were evaluated by the method of block averages.[9,34]

**Brownian Dynamics Simulations.** The torsional fluctuations in the equivalent anharmonic WLR were studied by Brownian dynamics (BD) simulations of a composite bead chain described earlier.[35] Every base pair was represented by a rigid composite bead of four virtual particles (Figure 1) labeled $O^i,X^i,Y^i,Z^i$ that form a rigid Cartesian frame. The upper indices

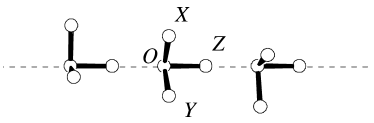


**Figure 1.** A discrete WLR model of a DNA fragment of three base pairs.

refer to the consecutive bead numbers in the chain. The total energy of an $N$-bead chain is composed of bond stretching, torsion, and bending terms as

$$H = \frac{h}{2}\sum_{i=1}^{N-1}(l_i - l_0)^2 + \sum_{i=1}^{N-1}U(\phi_i) + \frac{g}{2}\sum_{i=1}^{N-2}\beta^2 \quad (1)$$

with the twisting potential defined as described further below. All other interactions between the beads can be neglected because we consider only short stiff chains that cannot loop. Here, $l_i$ is the distance between particles $O^i$ and $O^{i+1}$, and $l_0$ is its equilibrium value. The $l_0$ value was 0.335 nm, corresponding to one base pair step. The torsion potential was applied to dihedral angles $\phi_i = X^iO^iO^{i+1}X^{i+1}$. In the bend energy term, the angular displacement was measured for angles $\beta = O^iO^{i+1}O^{i+2}$.

The DNA elasticity is conveniently characterized by three persistence lengths corresponding to bending, twisting, and stretching that we denote as $l_b$, $l_t$, and $l_s$, respectively. Parameters $g$ and $h$ in eq 1 were chosen so that the $l_b$ and $l_s$ values were similar in BD and MD. The energy coefficients were first estimated analytically and then verified by processing the resulting BD trajectories with previously described procedures.[35,36] For bending, we applied $l_b$ = 73 nm. For stretching, the value $l_s$ = 100 nm was used, corresponding to the Young's modulus $Y_f$ = 1410 pN. The BD simulation algorithm was considered in detail earlier.[35] It is based on the previous results of different groups.[37−41] For better comparison with atom-level MD, we considered short chains of 14 composite beads, computed BD trajectories of 164 ns with a time step of 0.5 ps, and saved chain configurations every 5 ps.

## RESULTS AND DISCUSSION

In the steady-stress all-atom MD simulations, the twisting torques are applied to terminal base pairs of a short fragment of a DNA double helix placed in a water box, so that the external torque at one end is compensated for by reactions at the opposite end and the integral external force and torque are always zero.[21] This algorithm can be viewed as if a demon in the moving global frame twists one end of the molecule and holds the opposite end so that the overall translation and rotation are not perturbed. For each value of the applied torque $\tau$, the steady-stress MD provides the equilibrium probability distribution $P_\tau(\Phi)$ of the twist $\Phi$ for one helical turn.[8,9] The two parameters corresponding to experimental observables are the average twist $\bar{\Phi}_\tau$ and the torsional persistence length $l_t(\tau) = L/\mathbf{D}_\tau[\Phi]$, where $L$ is the length of DNA and $\mathbf{D}_\tau[\Phi]$ is the variance of $P_\tau(\Phi)$. We are looking for a WLR model that would be indistinguishable from MD as regards these two observables, that is, this model should reproduce the torque dependences $\bar{\Phi}_\tau$ and $l_t(\tau)$ obtained by MD. In the harmonic approximation, the local potential is defined by only two parameters that can be computed directly from any pair of $\bar{\Phi}$ and $l_t$.[2] In our case, this


dx.doi.org/10.1021/jp311408h | J. Phys. Chem. B 2013, 117, 1857−1861

problem cannot be solved analytically; therefore, we approximated the single-step WLR twisting potential $U(\phi)$ by a polynomial

$$U(\phi) = q_1\phi + q_2\frac{1}{2}\phi^2 + q_3\frac{1}{6}\phi^3 + q_4\frac{1}{24}\phi^4 \quad (2)$$

and numerically fitted the coefficients $q_i$ to reproduce the MD data. For any trial potential, the twist probability distribution $p(\phi)$ and the partition function $Z$ are computed using the Boltzmann formula

$$p(\phi) = e^{-U(\phi)/kT} \qquad Z = \int_\phi p(\phi)\, d\phi \quad (3)$$

The required averages are obtained as

$$\langle\phi\rangle = \frac{1}{Z}\int_\phi p(\phi)\, d\phi \qquad D = \langle\phi^2\rangle - \langle\phi\rangle^2 \quad (4)$$

and these values are fit to MD data by nonlinear optimization in the space of coefficients $q_i$ of eq 2. These fitting procedures are discussed in detail in the Supporting Information. The resulting potential is referred to below as potential A.

The quality of fitting is demonstrated in Figure 2. It displays the input MD data and the analytical curves obtained by using

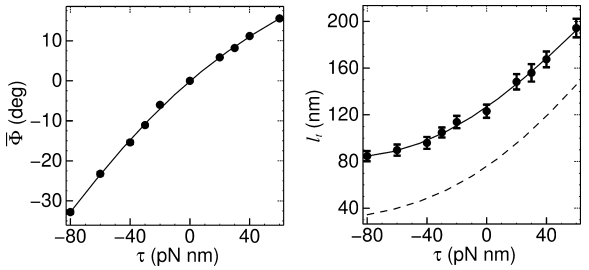


**Figure 2.** Variation of the average twist (left panel) and torsional persistence length (right panel) with the value of the external torque. The input MD data[9] are shown by circles, with statistical errors evaluated by block averages. Angle $\bar{\Phi}$ was measured and computed for one helical turn (11 bps). $\Phi = 0$ corresponds to the average twist in MD with $\tau = 0$. The analytical plots computed for potential A are shown by solid lines. The dashed plot in the right panel displays the analytical dependence for potential B fitted with the same input data scaled to compensate for the difference between MD and experiment.

eqs 3 and 4 with optimized coefficients in eq 2. It is seen that potential A accurately reproduces the MD results. This was additionally checked by BD simulations of the corresponding discrete WLR model. Figure 3 shows the computed BD distributions of torsional fluctuations with three contrasting values of external torques. The results are displayed for one bps (upper panel) and for one helical turn (lower panel). It is seen that potential A indeed determines a WLR model that reproduces the statistics of torsional fluctuations in all-atom DNA. Note that only the average MD data from Figure 2 were used for fitting. The good agreement of the shapes of BD and MD distributions in the lower panel of Figure 3 indicates a broader qualitative agreement.

Figure 4 compares the experimental and theoretical temperature dependences of the average helical twist. They all look as straight lines, although the theoretical plots are nonlinear curves computed by using eqs 3 and 4 for 100 temperatures evenly spaced in the given interval. It is seen that the WLR model with potential A predicts the thermal untwisting effect comparable to experiment, but the temperature coefficient is somewhat

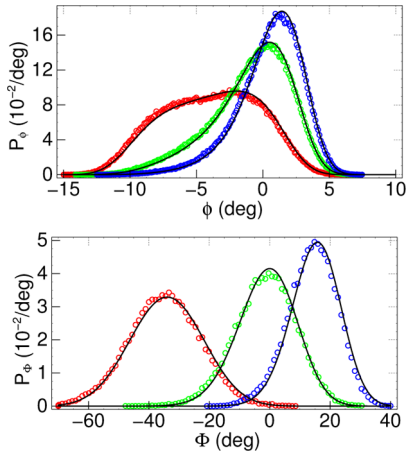


**Figure 3.** The results of BD simulations of the dodecamer WLR model with potential A (open circles). The twist probability distributions are shown for $\tau = -80$, 0, and +60 pN nm (from left to right) for one bps (upper panel) and for one helical turn of DNA (11 bps, lower panel). In the upper panel, the smooth lines show analytical distributions computed by eq 3 for potential A. In the lower panel, the smooth curves approximate with very high accuracy the raw MD distributions by using a similarly fitted torsional potential from our previous study.[42]

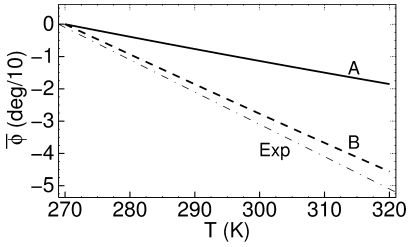


**Figure 4.** Comparison of experimental thermal untwisting with predictions of anharmonic twisting potentials. The experimental dependence (lower dashed−dotted line) represents a linear decrease with a temperature coefficient of 0.01°/K. The other two plots are labeled according to the text. For convenience, all plots are shifted to $\bar{\phi} = 0$ at $T = 270$ K.

smaller. One can reasonably ask whether this difference is significant in terms of the present approach. We decided to look for a modification of potential A that would reduce this discrepancy. The current all-atom MD models of DNA are torsionally more rigid than in reality.[42] For a less rigid model, with a similar anharmonicity, this temperature dependence may be steeper, that is, the difference between plot A and the experimental line in Figure 4 may be due to the same inaccuracy of all-atom potentials that gives an overestimated twisting rigidity. To check this possibility, the MD data were scaled by shifting the input dependence $l_t(\tau)$ uniformly to obtain $l_t(0) = 75$ nm, and the scaled data were used for fitting the coefficients in eq 2. The results for this new potential (potential B) are shown in Figures 2 and 4 by dashed lines. As expected, in the right panel of Figure 2, the profile of $l_t(\tau)$ for potential B is shifted vertically by a nearly constant value from the original MD data, with $l_t(0)$ similar to experiment. Interestingly, the thermal untwisting predicted by potential B is also very close to the experimental dependence (see Figure 4).

The profiles of potentials A and B are compared in Figure 5. Both of them are strongly anharmonic. Potential B has an evident double-well character, with a plateau in the region of


dx.doi.org/10.1021/jp311408h | J. Phys. Chem. B 2013, 117, 1857−1861

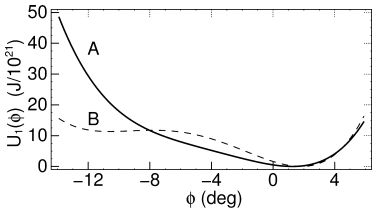


**Figure 5.** Comparison of the profiles of two fitted anharmonic potentials. The lines are labeled according to the text.

lower twists. This feature appears quite persistent. We varied the coefficients in eq 2 systematically and checked the profiles of the plots like those in Figures 2, 4, and 5. It appeared that the dependences close to MD and experiment are obtained only for WLR models with a pronounced double-well character of the twisting potential. The Boltzmann averaging predicts very minute untwisting even for strongly anharmonic potentials, and the seemingly small experimental temperature coefficient actually corresponds to a very significant anharmonicity. At the same time, the shape of potential B in Figure 5 does not contradict experimental data. It is known that in B-DNA, the C2′-endo conformation of the furanose can temporarily switch to the C3′-endo conformation corresponding to the A-form with a lower twist[43] There are also frequent twist-increasing transitions of adjacent $\varepsilon$ and $\zeta$ torsions from the BI to BII conformation.[44,45] These three substates are separated by small energy barriers, and they can account for the twist difference of several degrees.

Figure 4 suggests that the entire magnitude of the thermal untwisting effect measured in experiments can well be due to the intrinsic anharmonicity of the torsional rigidity of DNA. This interpretation implies that the type of anharmonicity inherent in GC-DNA, that is, the growth of $l_t$ with twisting, is typical for random sequences. Earlier FPA studies of supercoiled plasmids revealed trends of both signs depending on conditions like the DNA sequence and ion concentrations.[10−13] In these experiments, however, small changes in superhelical density sometimes resulted in very strong modulations of the torsional rigidity that cannot be compared with the effect considered here. It was suggested earlier[10,46] that the measured FPA signal depends on the overall plasmid structure through parameters involved in the data processing, notably, the angle between the intercalating dye and the DNA axis or the effective DNA diameter. Additional studies are needed to check this.

On the other hand, a qualitatively different anharmonicity observed in MD for AT-DNA[9] at closer inspection does not seem to be a contradiction. Figure 6 shows the results of three series of simulations, one for AT-DNA and two for GC-DNA (using different force fields). For GC-DNA, the earlier data[9] were supplemented by additional computations with the recent version of the AMBER force field parameters.[26] In the left panel, the three dependences look different. Notably, the AT-DNA rigidity decreases with small positive torques. However, when the same data are plotted with respect to the helical pitch (right panel), the three plots converge for pitches below 10.7. This surprising observation suggests that the behavior of $l_t$ is linked to the pitch and that for pitches around the experimental value for B-DNA in solution (10.5), the $l_t$ value usually grows with twisting. In this case, averaging over random sequences should give the anharmonicity similar to that in MD of GC-DNA because it has the equilibrium pitch close to 10.5.

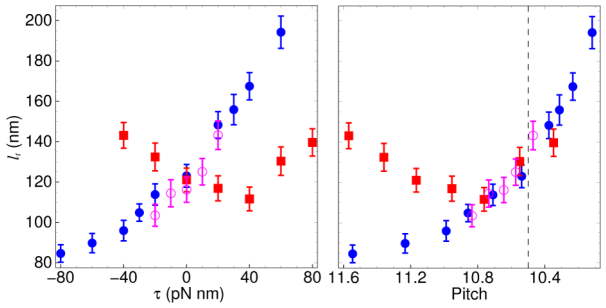


**Figure 6.** The DNA torsional persistence length plotted versus the applied torque (left panel) and the average helical pitch (right panel). The results are shown for AT-DNA (squares) and GC-DNA (circles). The two plots for GC-DNA were obtained with parm98[22,23] (closed circles) and bsc0$_{\chi OL4}$[24−26] (open circles) AMBER parameter sets. The vertical dashed line in the right panel marks the experimental pitch value of random DNA.

## CONCLUSION

The present paper proposes a new explanation of the phenomenon of thermal untwisting of the double-helical DNA. This strange effect was discovered experimentally nearly 40 years ago.[14−16] Here, it is shown that the thermal untwisting can be predicted from the specific anharmonicity of the torsional rigidity of the double helix revealed in the recent computational studies.[8,9] The effective twisting potential nearly quantitatively accounts for the thermal untwisting observed in experiments. These results confirm that the torsional rigidity of DNA is strongly anharmonic and that for random DNA, its value grows with small twisting and decreases with untwisting.

## ASSOCIATED CONTENT

### Supporting Information

The algorithm of fitting of the coarse-grained twisting potentials and the numerical results of the fitting. This material is available free of charge via the Internet at http://pubs.acs.org/.

## AUTHOR INFORMATION

### Corresponding Author

*E-mail: alexey@ibpc.fr.

### Notes

The authors declare no competing financial interest.

## REFERENCES

(1) Chow, K. L.; Hogan, M. E.; Schwartz, R. J. *Proc. Natl. Acad. Sci. U.S.A.* **1991**, *88*, 1301−1305.
(2) Allison, S.; Austin, R.; Hogan, M. *J. Chem. Phys.* **1989**, *90*, 3843−3854.
(3) Marko, J. F.; Siggia, E. D. *Macromolecules* **1994**, *27*, 981−988.
(4) Marko, J. F. *Europhys. Lett.* **1997**, *38*, 183−188.
(5) Kamien, R. D.; Lubensky, T. C.; Nelson, P.; O'Hern, C. S. *Europhys. Lett.* **1997**, *38*, 237−242.
(6) Gore, J.; Bryant, Z.; Nollmann, M.; Le, M. U.; Cozzarelli, N. R.; Bustamante, C. *Nature* **2006**, *442*, 836−839.
(7) Lionnet, T.; Joubaud, S.; Lavery, R.; Bensimon, D.; Croquette, V. *Phys. Rev. Lett.* **2006**, *96*, 178102.
(8) Mazur, A. K. *Phys. Rev. Lett.* **2010**, *105*, 018102.
(9) Mazur, A. K. *Phys. Rev. E* **2011**, *84*, 021903.
(10) Shibata, J. H.; Wilcoxon, J.; Schurr, J. M.; Knauf, V. *Biochemistry* **1984**, *23*, 1188−1194.
(11) Song, L.; Fujimoto, B. S.; Wu, P. G.; Thomas, J. C.; Shibata, J. H.; Schurr, J. M. *J. Mol. Biol.* **1990**, *214*, 307−326.

(12) Selvin, P. R.; Cook, D. N.; Pon, N. G.; Bauer, W. R.; Klein, M. P.; Hearst, J. E. *Science* **1992**, *255*, 82−85.
(13) Heath, P. J.; Clendenning, J. B.; Fujimoto, B. S.; Schurr, J. M. *J. Mol. Biol.* **1996**, *260*, 718−30.
(14) Wang, J. C. *J. Mol. Biol.* **1969**, *43*, 25−39.
(15) Pulleyblank, D. E.; Shure, M.; Tang, D.; Vinograd, J.; Vosberg, H. P. *Proc. Natl. Acad. Sci. U.S.A.* **1975**, *72*, 4280−4284.
(16) Duguet, M. *Nucleic Acids Res.* **1993**, *21*, 463−8.
(17) Peck, L. J.; Wang, J. C. *Nature* **1981**, *292*, 375−378.
(18) Lee, C.-H.; Mizusawa, H.; Kakefuda, T. *Proc. Natl. Acad. Sci. U.S.A.* **1981**, *78*, 2838−2842.
(19) Vinograd, J.; Greenwald, R.; Hearst, J. E. *Biopolymers* **1965**, *3*, 109−114.
(20) Mazur, A. K. *ChemPhysChem* **2008**, *9*, 2691−2694.
(21) Mazur, A. K. *J. Chem. Theory Comput.* **2009**, *5*, 2149−2157.
(22) Cornell, W. D.; Cieplak, P.; Bayly, C. I.; Gould, I. R.; Merz, K. M.; Ferguson, D. M.; Spellmeyer, D. C.; Fox, T.; Caldwell, J. W.; Kollman, P. A. *J. Am. Chem. Soc.* **1995**, *117*, 5179−5197.
(23) Cheatham, T. E., III; Cieplak, P.; Kollman, P. A. *J. Biomol. Struct. Dyn.* **1999**, *16*, 845−862.
(24) Wang, J.; Cieplak, P.; Kollman, P. A. *J. Comput. Chem.* **2000**, *21*, 1049−1074.
(25) Perez, A.; Marchan, I.; Svozil, D.; Sponer, J.; Cheatham, T. E.; Laughton, C. A.; Orozco, M. *Biophys. J.* **2007**, *92*, 3817−3829.
(26) Krepl, M.; Zgarbova, M.; Stadlbauer, P.; Otyepka, M.; Banas, P.; Koca, J.; Cheatham, T. E.; Jurecka, P.; Sponer, J. *J. Chem. Theory Comput.* **2012**, *8*, 2506−2520.
(27) Essmann, U.; Perera, L.; Berkowitz, M. L.; Darden, T.; Lee, H.; Pedersen, L. G. *J. Chem. Phys.* **1995**, *103*, 8577−8593.
(28) Berendsen, H. J. C.; Postma, J. P. M.; van Gunsteren, W. F.; DiNola, A.; Haak, J. R. *J. Chem. Phys.* **1984**, *81*, 3684−3690.
(29) Mazur, A. K. *J. Comput. Chem.* **1997**, *18*, 1354−1364.
(30) Mazur, A. K. *J. Chem. Phys.* **1999**, *111*, 1407−1414.
(31) Mazur, A. K. *J. Am. Chem. Soc.* **1998**, *120*, 10928−10937.
(32) Mazur, A. K. *J. Phys. Chem. B* **1998**, *102*, 473−479.
(33) Mazur, A. K. *Biophys. J.* **2006**, *91*, 4507−4518.
(34) Flyvbjerg, H.; Petersen, H. G. *J. Chem. Phys.* **1989**, *91*, 461−466.
(35) Mazur, A. K. *J. Phys. Chem. B* **2009**, *113*, 2077−2089.
(36) Mazur, A. K. *J. Phys. Chem. B* **2008**, *112*, 4975−4982.
(37) Ermak, D. L.; McCammon, J. A. *J. Chem. Phys.* **1978**, *69*, 1352−1360.
(38) Allison, S. A. *Macromolecules* **1986**, *19*, 118−124.
(39) Iniesta, A.; de la Torre, J. G. *J. Chem. Phys.* **1990**, *92*, 2015−2018.
(40) Chirico, G.; Langowski, J. *Macromolecules* **1992**, *25*, 769−775.
(41) Jian, H.; Schlick, T.; Vologodskii, A. *J. Mol. Biol.* **1998**, *284*, 287−296.
(42) Mazur, A. K. *Phys. Rev. E* **2012**, *86*, 011914.
(43) Thomas, G. A.; Peticolas, W. L. *J. Am. Chem. Soc.* **1983**, *105*, 993−996.
(44) Fratini, A. V.; Kopka, M. L.; Drew, H. R.; Dickerson, R. E. *J. Biol. Chem.* **1982**, *257*, 14686−14707.
(45) Heddi, B.; Oguey, C.; Lavelle, C.; Foloppe, N.; Hartmann, B. *Nucleic Acids Res.* **2010**, *38*, 1034−47.
(46) Millar, D. P.; Robbins, R. J.; Zewail, A. H. *J. Chem. Phys.* **1982**, *76*, 2080−2094.